広島大学学術情報リポジトリ
Hiroshima University Institutional Repository

Title	Solvent Effects on the Encapsulation of Divalent Ions by Benzo-18-Crown-6 and Benzo-15-Crown-5
Author(s)	Inokuchi, Yoshiya; Ebata, Takayuki; Rizzo, Thomas R.
Citation	Journal of Physical Chemistry A , 119 (29) : 8097 - 8105
Issue Date	2015-07-23
DOI	10.1021/acs.jpca.5b04450
Self DOI	
URL	https://ir.lib.hiroshima-u.ac.jp/00046470
Right	Copyright (c) 2015 American Chemical Society This document is the Accepted Manuscript version of a Published Work that appeared in final form in Journal of Physical Chemistry A, copyright © American Chemical Society after peer review and technical editing by the publisher. To access the final edited and published work see https://doi.org/10.1021/acs.jpca.5b04450.
Relation	

Solvent Effects on the Encapsulation of Divalent Ions by Benzo-18-Crown-6 and Benzo-15-Crown-5

Yoshiya Inokuchi,[‡,*] Takayuki Ebata,[‡] and Thomas R. Rizzo[†]

Department of Chemistry, Graduate School of Science, Hiroshima University, Higashi-Hiroshima, Hiroshima 739-8526, Japan and Laboratoire de Chimie Physique Moléculaire, École Polytechnique Fédérale de Lausanne, Lausanne CH-1015, Switzerland

E-mail: y-inokuchi@hiroshima-u.ac.jp

Abstract

We measure UV photodissociation (UVPD) spectra of cold benzo-15-crown-5 (B15C5) and benzo-18-crown-6 (B18C6) complexes with divalent ions (M^{2+} = Ca^{2+}, Sr^{2+}, Ba^{2+}, and Mn^{2+}), solvated with an H_2O or a CH_3OH molecule: M^{2+}•B15C5•H_2O, M^{2+}•B15C5•CH_3OH, M^{2+}•B18C6•H_2O, and M^{2+}•B18C6•CH_3OH. All the species show a number of sharp vibronic bands in the 36600–37600 cm^{-1} region, which can be attributed to electronic transitions of the B18C6 or B15C5 component. Conformer-specific IR spectra of these complexes are also obtained by IR-UV double-resonance spectroscopy in the OH stretching region. All the IR-UV spectra of the H_2O complexes show IR bands at ~3610 and ~3690 cm^{-1}; these bands can be assigned to the symmetric and asymmetric OH stretching vibrations of the H_2O component. The CH_3OH complexes also show the stretching vibration of the OH group at ~3630 cm^{-1}. The H_2O and the CH_3OH components are directly bonded to the

M^{2+} ion through the M^{2+}•••O bond in all the complexes, but a small difference in the conformation results in a noticeable difference in the OH stretching frequency, which enables us to determine the number of conformers. For Ca^{2+}, Sr^{2+}, and Mn^{2+}, the number of conformers for the B18C6 complexes is in the range of 2–5, which is clearly larger than complexes with B15C5 (1 or 2). However for Ba^{2+}, the number of conformers with B18C6 (1 or 2) is almost the same as that with B15C5. This is probably because the Ba^{2+} ion is too large to be located in the cavity center of either B15C5 and B18C6, which provides an open site at the Ba^{2+} ion suitable for solvation with H_2O or CH_3OH. The more conformations a complex can take, the more entropically favored it is at non-zero temperatures. Hence, the larger number of conformations suggests higher stability of the complexes under solvated conditions, leading to a higher degree of ion encapsulation in solution.

Keywords: alkaline earth, transition metal, 18-crown-6, 15-crown-5, encapsulation, water, crown ether, infrared, ion trap, electrospray, solvent effect, ultraviolet, conformation

*To whom correspondence should be addressed.

[‡]Hiroshima University

[†]École Polytechnique Fédérale de Lausanne

1. Introduction

It is well known that crown ethers show ion selectivity in solution.[1,2] This has been explained mainly by the optimal matching in size between the crown cavity and the ion.[1,3] The crystal structure of host-guest complexes was extensively examined by X-ray diffraction.[1,3] However, it is not so obvious how the matching in size controls the efficiency of the encapsulation in solution. Mass spectrometric and theoretical studies of metal ion-crown ether complexes in the gas phase have demonstrated that the binding energy between the crowns and the metal ions (for example, 18-crown-6 and alkali metal ions) is larger for smaller ions,[4-27] and that solvent effects play important roles for the ion selectivity of crown ethers in solution.[10-12,21] Lisy and co-workers measured IR photodissociation (IRPD) spectra of alkali metal ions with 18-crown-6 and H_2O molecules and determined the complex structure by comparing the IRPD spectra with calculated spectra.[28,29] They suggested that several conformers coexist for each complex, but it was not easy to determine the number of conformers and their structures definitely from the IRPD spectra. Martínez–Haya, Oomens, and their coworkers reported IR multiple photon dissociation spectroscopy of divalent metal ion-crown ether complexes.[30-32] A remarkable shift of the C–O stretching band is seen for 18-crown-6 complexes with alkaline earth metal cations in comparison to alkali metal cation complexes. This shift is ascribed to stronger binding of alkaline earth metal cations to the oxygen atoms and to the degree of folding of 18-crown-6.[32] Kim, Heo, and their coworkers studied ultraviolet photodepletion spectroscopy of dibenzo-18-crown-6 complexes with alkaline earth metal divalent cations.[33] More recently, we have applied UV photodissociation (UVPD) and IR-UV double-resonance spectroscopy to cold dibenzo-18-crown-6 complexes (DB18C6) with alkali metal ions and H_2O molecules, M^+•DB18C6•$(H_2O)_{1-5}$.[34] We determined the

structure and the number of conformers on the basis of the IR spectra and discussed the selectivity of encapsulation of ions by the crown ethers in solution in terms of entropic effects related to the number of conformers.

In the present work, we investigate UV and IR spectroscopy of cold complexes of benzo-15-crown-5 (B15C5) and benzo-18-crown-6 (B18C6) with divalent ions, solvated by one H_2O or CH_3OH molecule: M^{2+}•B15C5•L and M^{2+}•B18C6•L (M^{2+} = Ca^{2+}, Sr^{2+}, Ba^{2+}, and Mn^{2+}, and L = H_2O and CH_3OH). We employ UVPD and IR-UV double resonance spectroscopy to measure UV spectra and conformer-selective IR spectra of the cold species in the OH stretching (3200–3800 cm^{-1}) region and determine the number of the conformers and their structure. We discuss the relation between the number of the conformers and the matching in size between the crown cavity and the metal ions.

2. Experimental and computational methods

The details of our experimental approach have been described previously.[34-36] Briefly, M^{2+}•B15C5•H_2O, M^{2+}•B15C5•CH_3OH, M^{2+}•B18C6•H_2O, and M^{2+}•B18C6•CH_3OH (M^{2+} = Ca^{2+}, Sr^{2+}, Ba^{2+}, and Mn^{2+}) complexes are produced continuously at atmospheric pressure *via* nanoelectrospray of a solution containing metal chloride and the crown ethers (~10 μM each) dissolved in methanol/water (~9:1 volume ratio). The parent ions of interest are selected in a quadrupole mass filter and injected into a 22-pole RF ion trap, which is cooled by a closed cycle He refrigerator to ~6 K. The trapped ions are themselves cooled internally and translationally to ~10 K through collisions with cold He buffer gas,[35-38] which is pulsed into the trap. The

trapped ions are then irradiated with a UV laser pulse, which causes some fraction of them to dissociate. The resulting charged photofragments, together with the remaining parent ions, are released from the trap, analyzed by a second quadrupole mass filter, and detected with a channeltron electron multiplier. Ultraviolet photodissociation (UVPD) spectra of parent ions are obtained by plotting the yield of a particular photofragment as a function of the wavenumber of the UV laser. For IR-UV double resonance spectroscopy, the output pulse of an IR OPO precedes the UV pulse by ~100 ns and counter-propagates through the 22-pole. Absorption of the IR light by ions in a specific conformational state warms them up, reducing the net UV absorption by this conformer.[39] The wavenumber of the UV laser is fixed to a vibronic transition of a specific conformer, and the wavenumber of the OPO is scanned in the OH stretching region (3200–3800 cm^{-1}) while monitoring the number of fragment ions. IR-UV depletion spectra are obtained by plotting the yield of a particular photofragment as a function of the OPO wavenumber. In the experiments of the Ca^{2+}, Sr^{2+}, and Ba^{2+} complexes, we examine the most abundant isotopomers having ^{40}Ca, ^{88}Sr, and ^{138}Ba.

We also perform quantum chemical calculations for all the complexes in this study. For geometry optimization of the Ca^{2+} complexes, we first use a classical force field to find conformational minima. The initial conformational search is performed by using the CONFLEX High Performance Conformation Analysis program with the MMFF94s force field.[40,41] The lowest energy conformers found with the force field calculations are then optimized at the M05-2X/6-31+G(d) level with *loose* optimization criteria using the GAUSSIAN09 program package.[42] The unique minima obtained by comparison of relative energies are further optimized using the M05-2X/6-31+G(d) basis set. Vibrational analysis is carried out for the optimized structures at the same computational level. In the CONFLEX software we cannot perform the

conformational search for the Sr^{2+} and Ba^{2+} complexes because the force field is not available for these ions. We thus produce initial conformations for the geometry optimization of the Sr^{2+} and Ba^{2+} complexes by replacing the Ca^{2+} ion in the geometry-optimized Ca^{2+} complexes with Sr^{2+} or Ba^{2+}. In the geometry optimization of the Sr^{2+} and Ba^{2+} complexes, we use the Stuttgart RLC ECP for Sr and Ba, and 6-31+G(d) for C, H, and O; functions of the ECPs are obtained from a database of basis sets.[43] For the Mn^{2+} complexes, we first use Ni^{2+} instead of Mn^{2+} to perform the initial conformational search, since the force field in the CONFLEX does not include Mn^{2+}. We then carry out geometry optimization with the GAUSSIAN09 program package by replacing the Ni^{2+} ion in the conformations with Mn^{2+}. The highest spin state (sextet) is much more stable than other spin states for the Mn^{2+} complexes; all the quantum chemical calculations are performed at the sextet spin state.

3. Results and Discussion

Figure 1 shows the UVPD spectra of (a) Ca^{2+}•B15C5•H_2O, (b) Ca^{2+}•B15C5•CH_3OH, (c) Ca^{2+}•B18C6•H_2O, and (d) Ca^{2+}•B18C6•CH_3OH in the 36600–37600 cm^{-1} region. Similarly, the UVPD spectra of the Sr^{2+}, Ba^{2+}, and Mn^{2+} complexes are displayed in Figs. 2a–d, 3a–d, 4a–d, respectively. These spectra are measured by monitoring the yield of the M^{2+}•B15C5 or M^{2+}•B18C6 photofragment. In our ion source we cannot produce enough bare M^{2+}•B15C5 or M^{2+}•B18C6 complexes for UVPD spectroscopy—at least one H_2O or CH_3OH molecule is always attached. The band origins of neutral B15C5 is found at 35645, 35653, and 36217 cm^{-1} for three conformers.[44] Neutral B18C6 shows the band origins at 35167 cm^{-1} and around 35650 cm^{-1} for four conformers.[45] Thus, all the UVPD spectra in Figs. 1–4 show blue-shifted

transitions compared to neutral B15C5 or B18C6; this is the same trend as that of B15C5 and B18C6 complexes with alkali metal ions.[46] All the UVPD spectra in Figs. 1–4 show a number of vibronically resolved bands. In order to distinguish vibronic bands due to different conformers and determine their structure, we measure the IR-UV spectra of the complexes by fixing the UV wavenumber at one of the vibronic bands and scanning the wavenumber of the IR OPO in the OH stretching region. In addition, we measure conformer-specific UVPD spectra by fixing the IR frequency to one of the vibrational bands of a particular conformer and scanning the UV frequency. By examining the depletion yield of each vibronic band by the IR excitation we can distinguish those bands in the UVPD spectra that belong to the same conformer. The UVPD spectra measured with IR excitation are shown in the Supporting Information (Figs. 1S–8S).

Figure 5a shows the IR-UV spectrum of the Ca^{2+}•B15C5•H_2O complex measured by monitoring the intensity of the vibronic band at 37105 cm^{-1} in Fig. 1a. Vibrational bands are observed at 3610 and 3676 cm^{-1}. Setting the UV laser on most of the strong vibronic bands in the UVPD spectrum of Ca^{2+}•B15C5•H_2O results in IR bands at the same positions as those in Fig. 5a. The UVPD spectrum with the IR excitation at 3610 cm^{-1} (Fig. 1S of the Supporting Information) shows uniform depletion for all the vibronic bands. These results indicate that there is only one conformer for the Ca^{2+}•B15C5•H_2O complex in our experiment. The calculated IR spectra and the optimized structures of the Ca^{2+}•B15C5•H_2O complex are displayed in Figs. 9S and 25S in the Supporting Information. All the calculated spectra display the symmetric and asymmetric OH stretching vibrations at similar positions (~3596 and ~3673 cm^{-1}, respectively); it is not possible to determine the structure of the Ca^{2+}•B15C5•H_2O complex definitely from the observed and calculated vibrational

spectrum alone. In all the calculated conformers, the H_2O molecule is directly attached to the Ca^{2+} ion through a Ca^{2+}•••O intermolecular bond; the two OH groups of the H_2O molecule are almost free from an intermolecular bond. The observed IR-UV bands at 3610 and 3676 cm^{-1} can be assigned to the symmetric and asymmetric OH stretching vibrations of the H_2O component. For the Ca^{2+}•B15C5•CH_3OH complex, the IR-UV measurement provides only one IR spectrum (Fig. 5b); there is also only one conformer for Ca^{2+}•B15C5•CH_3OH in our experiment. The IR band observed at 3641 cm^{-1} is assigned to the OH stretching vibration of CH_3OH. The calculated IR spectra and the optimized structures of Ca^{2+}•B15C5•CH_3OH are shown in Figs. 10S and 26S. All the conformers have CH_3OH bound to the Ca^{2+} ion and an OH stretching band at almost the same frequency (~3636 cm^{-1}). Again, it is difficult to determine the conformer structure by comparison of the observed and calculated IR spectra, but it is likely that CH_3OH is directly bonded to the Ca^{2+} ion through a Ca^{2+}•••O bond and that the OH group is free from an intermolecular bond.

In contrast to the case of the Ca^{2+}•B15C5•H_2O and Ca^{2+}•B15C5•CH_3OH complexes, the B18C6 complexes of Ca^{2+} ion show multiple conformations. Figure 5c displays the IR-UV spectra of the Ca^{2+}•B18C6•H_2O complex. All the IR-UV spectra show the bands at similar positions (~3615 and ~3695 cm^{-1}), but noticeable differences in the frequencies can be seen among the three spectra. The IR-UV spectrum measured at 36951 cm^{-1} (the upper spectrum in Fig. 5c) has both gain and depletion signals around 3615 and 3695 cm^{-1}. The UV band at 36951 cm^{-1} (band (3) in Fig. 1c) is relatively weaker than the other bands. In the IR-UV measurement at 36951 cm^{-1}, electronic transitions from vibrationally excited states of main conformers also occur and provide the same photofragment Ca^{2+}•B18C6 ion. This excitation process gives gain signals in the IR-UV spectrum of the minor conformer measured at 36951 cm^{-1}.[35,46]

From the IR-UV results in Fig. 5c, we conclude that the Ca^{2+}•B18C6•H_2O complex has at least three conformers in our experiment. The IR bands around 3615 and 3695 cm^{-1} can be assigned to the symmetric and asymmetric OH stretching vibrations of H_2O. The calculated IR spectra and the optimized structures are shown in Figs. 11S and 27S in the Supporting Information. Because all the calculated isomers have IR bands close to each other, it is difficult to determine the conformer structure from the IR spectra. However, it is likely that H_2O is directly attached to Ca^{2+} in all the three conformers in the experiment. In the case of the Ca^{2+}•B18C6•CH_3OH complex, three types of IR-UV spectra are also observed in the OH stretching region (Fig. 5d). The IR bands of the Ca^{2+}•B18C6•CH_3OH ion in Fig. 5d are assigned to the OH stretching vibration. The position of the IR bands of the three conformers is close to each other, indicating the similarity of their structures.

Figures 6a–d, 7a–d, and 8a–d show the IR-UV spectra of the Sr^{2+}, Ba^{2+}, and Mn^{2+} complexes, respectively. All the complexes show OH stretching vibrations in the 3550–3700 cm^{-1} region. The IR bands of the H_2O complexes at ~3600 and ~3680 cm^{-1} are attributed to the symmetric and asymmetric OH stretching vibrations of the H_2O component, respectively. The band in the IR spectra of the methanol complexes is due to the OH stretching vibration of methanol. Based on their stretching frequencies, the OH groups are free from a strong intermolecular bond, and the H_2O or CH_3OH is bound to the M^{2+} ion through an M^{2+}•••O bond. The IR-UV spectrum of the Sr^{2+}•B15C5•CH_3OH complex is expanded around 3640 cm^{-1} (Fig. 6b). Though the difference in the OH frequency is quite small (~1.1 cm^{-1}), they are reproducibly different; there are at least two conformers for Sr^{2+}•B15C5•CH_3OH. Similar to the case of the Ca^{2+}•B18C6•H_2O complex (Fig. 5c), the Ba^{2+}•B18C6•CH_3OH ion also shows a gain-dip feature around 3644 cm^{-1} (Fig. 7d). The gain and depletion signals are

attributed to a main and a minor conformer, respectively. For the B15C5 complexes, the OH bands appear at ~3610 and ~3677 cm^{-1} for the H_2O complexes and at ~3640 cm^{-1} for the CH_3OH complexes, except for band (1) of Ba^{2+}•B15C5•H_2O (Fig. 7a). This conformer shows OH bands at 3587 and 3670 cm^{-1}, which are smaller than those of the other B15C5•H_2O complexes; it is probable that the OH groups are bonded to the benzene ring of B15C5 through the O–H•••π hydrogen bonds. The Mn^{2+}•B15C5•H_2O and Mn^{2+}•B15C5•CH_3OH complexes have only one isomer each (Figs. 8a and 8b). In contrast to the B15C5 complexes, those containing B18C6 show a wider range of OH frequencies for Ca^{2+}, Sr^{2+}, Ba^{2+}, and Mn^{2+}. The symmetric and asymmetric OH stretching frequencies of the H_2O component are in the range of 3583–3616 and 3674–3699 cm^{-1}, respectively. The OH bands of the CH_3OH complexes are located in the 3598–3646 cm^{-1} range. The difference in the OH frequencies reflects the orientation of the H_2O or CH_3OH component against the metal ion-crown ether complexes. The B18C6 complexes can have more different types of solvation geometries than those with B15C5.

We collect the number of conformers determined by IR-UV double-resonance spectroscopy in Table 1. The number of conformers of the B18C6 complexes is obviously larger than that of the B15C5 complexes for Ca^{2+}, Sr^{2+}, and Mn^{2+} ions. For instance, the number of conformers of the Ca^{2+}•B18C6•H_2O complex (3) is larger than that of the Ca^{2+}•B15C5•H_2O complex (1). In contrast, the Ba^{2+} complexes do not show such a clear trend—the Ba^{2+}•B15C5•CH_3OH and Ba^{2+}•B18C6•CH_3OH complexes have one and two conformation(s), respectively, whereas the Ba^{2+}•B15C5•H_2O and Ba^{2+}•B18C6•H_2O complexes have two and one conformer(s). These results can be attributed to the matching in size between the crown cavity and the metal ions, as seen

in the case of the K^+•DB18C6•$(H_2O)_3$, Rb^+•DB18C6•$(H_2O)_3$, and Cs^+•DB18C6•$(H_2O)_3$ complexes.[34] The cavity size of DB18C6 shows an optimum matching with K^+ ion among alkali metal ions; the K^+ ion in the K^+•DB18C6 complex is located almost at the center of the DB18C6 cavity. In this case, the H_2O molecules can be bound to the K^+ ion directly from both top and bottom of the DB18C6 cavity, providing multiple hydration forms. In contrast, the Rb^+ or Cs^+ ion is located slightly out of the cavity in the DB18C6 complexes, because these ions are too big to be located at the center. Here the hydration to the metal ions is possible only from the top, giving only one conformation. Coming back to the alkali earth metal ions, Figs. 9 and 10 show the most stable structures of the B15C5 and B18C6 complexes, respectively. In the bare complexes of B15C5 with Ca^{2+}, Sr^{2+}, and Ba^{2+} (Fig. 9), the B15C5 cavity is too small to encapsulate these ions completely; one side of the metal ions is open for direct solvation. The H_2O or CH_3OH molecule is bound on the open side, opposite to the B15C5. This situation is quite similar to the Rb^+•DB18C6 and Cs^+•DB18C6 complexes.[34] In contrast, the B18C6 component in the bare complexes holds the Ca^{2+}, Sr^{2+}, and Ba^{2+} ions more deeply than B15C5 (Fig. 10). In the solvated complexes, the H_2O or CH_3OH molecule tends to extract the metal ions from the crown cavity by being attached directly to the metal ions through the M^{2+}•••O bond. Figure 11 shows the distance between the mean plane of the crown oxygen atoms and the metal ion in the complexes as a function of the ionic radii of the M^{2+} ions. The ionic radii of Ca^{2+}, Sr^{2+}, Ba^{2+}, and Mn^{2+} were reported to be 1.00, 1.18, 1.35, and 0.83 Å, respectively, with a coordination number of 6 in crystals.[47] In the case of the bare B15C5 complexes (Fig. 11a), the distance increases from 0.77 to 1.37 Å with increasing the ion size for Ca^{2+}, Sr^{2+}, and Ba^{2+}. Attachment of one H_2O or CH_3OH molecule does not elongate the distance so much. As seen in Fig. 9, the top side of the bare M^{2+}•B15C5 complexes is open for

solvation. The solvent H_2O or CH_3OH molecule is attached on that side, forming one or a few stable conformer(s). For the bare M^{2+}•B18C6 complexes, the distance of Ca^{2+} and Sr^{2+} (0.11 and 0.15 Å) is shorter than those of the B15C5 complexes as well as that of K^+•B18C6 (~0.20 Å), which is thought to have an optimum matching in size between K^+ and B18C6.[42] However, attachment of only one solvent molecule extracts the metal ion significantly, by ~0.3 Å on average; the metal ion in the solvated Ca^{2+}•B18C6 and Sr^{2+}•B18C6 complexes can be located in a bigger space than the B15C5 complexes. This results in the existence of multiple conformers for the Ca^{2+}•B18C6 and Sr^{2+}•B18C6 systems. In the bare Ba^{2+}•B18C6 complex, the distance (0.25 Å) is larger than that of the Ca^{2+}, Sr^{2+}, and K^+ complexes. The Ba^{2+} ion is encapsulated by B18C6 less deeply than Ca^{2+}, Sr^{2+}, and K^+, which results in a smaller number of conformers for the solvated Ba^{2+}•B18C6 complexes, similar to the case of the M^{2+}•B15C5 complexes described above. In the case of the Mn^{2+} complexes, the distance of the Mn^{2+}•B15C5 ion (0.06 Å) is almost the same as that of Mn^{2+}•B18C6 (0.07 Å). However, the attachment of one H_2O or CH_3OH molecule elongates the distance by ~0.41 Å in the latter complex, which is more than in the former (~0.27 Å). Also for the Mn^{2+} ion, B18C6 allows larger flexibility of the metal position in the solvated complexes than B15C5, which provides more conformations for B18C6. From a thermochemical point of view, a larger number of conformations can provide larger stability in solution. In the encapsulation systems where an optimal matching in size occurs between host and guest species, there can be some flexibility in the position of the guest against the host. As a result, a larger number of solvation manners become possible for such systems when it is dissolved, which enhances the capability of encapsulation in solution.

4. Summary

We have measured the UV photodissociation (UVPD) and IR-UV double resonance spectra of the M^{2+}•B15C5•H_2O, M^{2+}•B15C5•CH_3OH, M^{2+}•B18C6•H_2O, and M^{2+}•B18C6•CH_3OH (M^{2+} = Ca^{2+}, Sr^{2+}, Ba^{2+}, and Mn^{2+}) complexes produced by nanoelectrospray and cooled to ~10 K in a 22-pole ion trap. The results of the IR-UV experiment suggest that the H_2O or CH_3OH molecule in these complexes is attached directly to the metal ions through the M^{2+}•••O bond. We have determined the number of conformers for these complexes on the basis of the IR-UV spectra. In the case of Ca^{2+}, Sr^{2+}, and Mn^{2+}, the number of conformations for the B18C6 complexes is larger than those with B15C5. In contrast, the Ba^{2+} ion has small number of conformers (one or two) for both of B15C5 and B15C5. These results indicate that the complexes with a good matching in size between the metal ion and the crown ether have a larger number of conformations under solvated conditions, which results in a higher degree of ion encapsulation in solution driven by entropic effects. The difference in the number of conformations of the different ion complexes is thus at the root of the selectivity of ion encapsulation.

Acknowledgment

This work is partly supported by the Swiss National Science Foundation through grant 200020_152804 and École Polytechnique Fédérale de Lausanne (EPFL). YI and TE thank the support from JSPS through the program “Strategic Young Researcher Overseas Visits Program for Accelerating Brain Circulation”.

Supporting Information Available: The UVPD spectra with the IR excitation, optimized structures and calculated IR spectra of the complexes, and a full list of authors of Ref. 42. This material is available free of charge *via* the internet at http://pubs.acs.org.

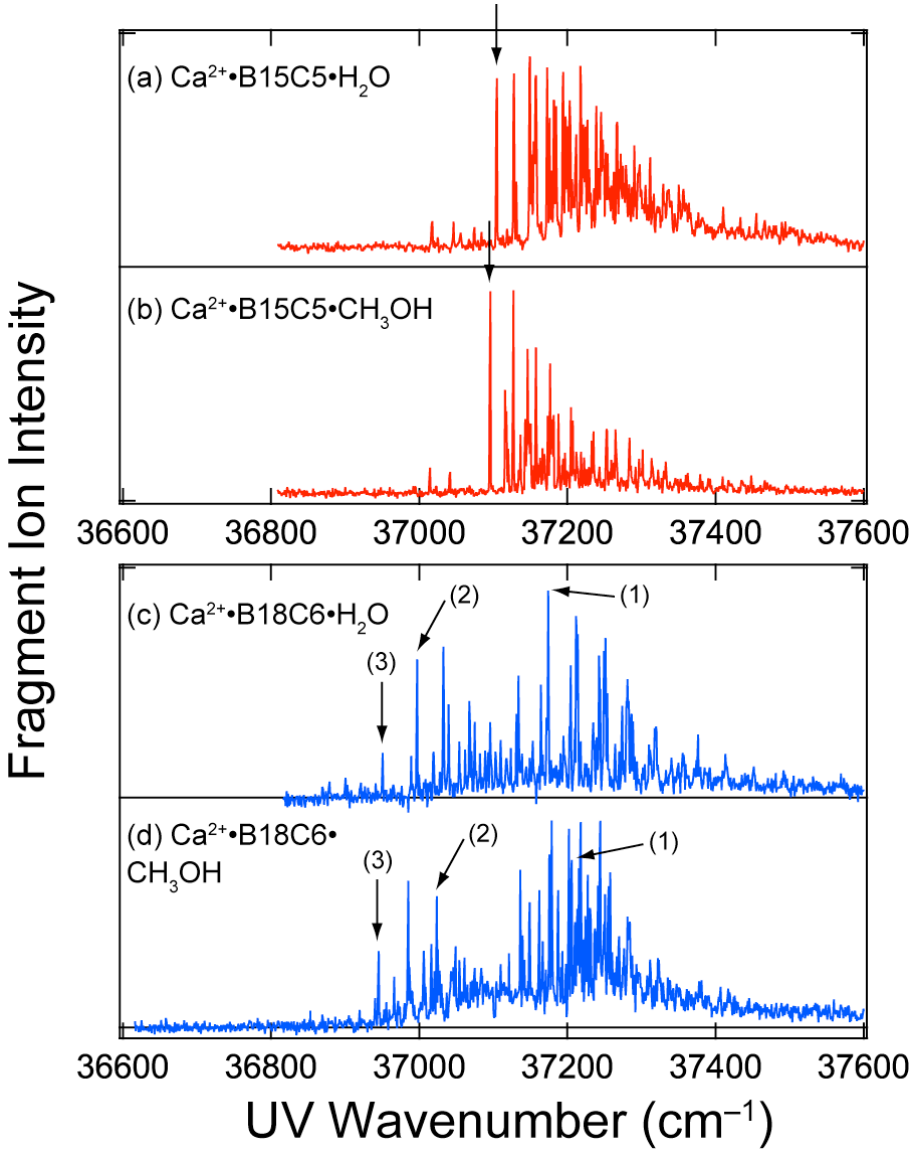

Figure 1. The UVPD spectra of the Ca^{2+} complexes. The arrows show the UV positions at which the IR-UV spectra are measured. The intensity of each spectrum is normalized as having the same maximum intensity for all the spectra.

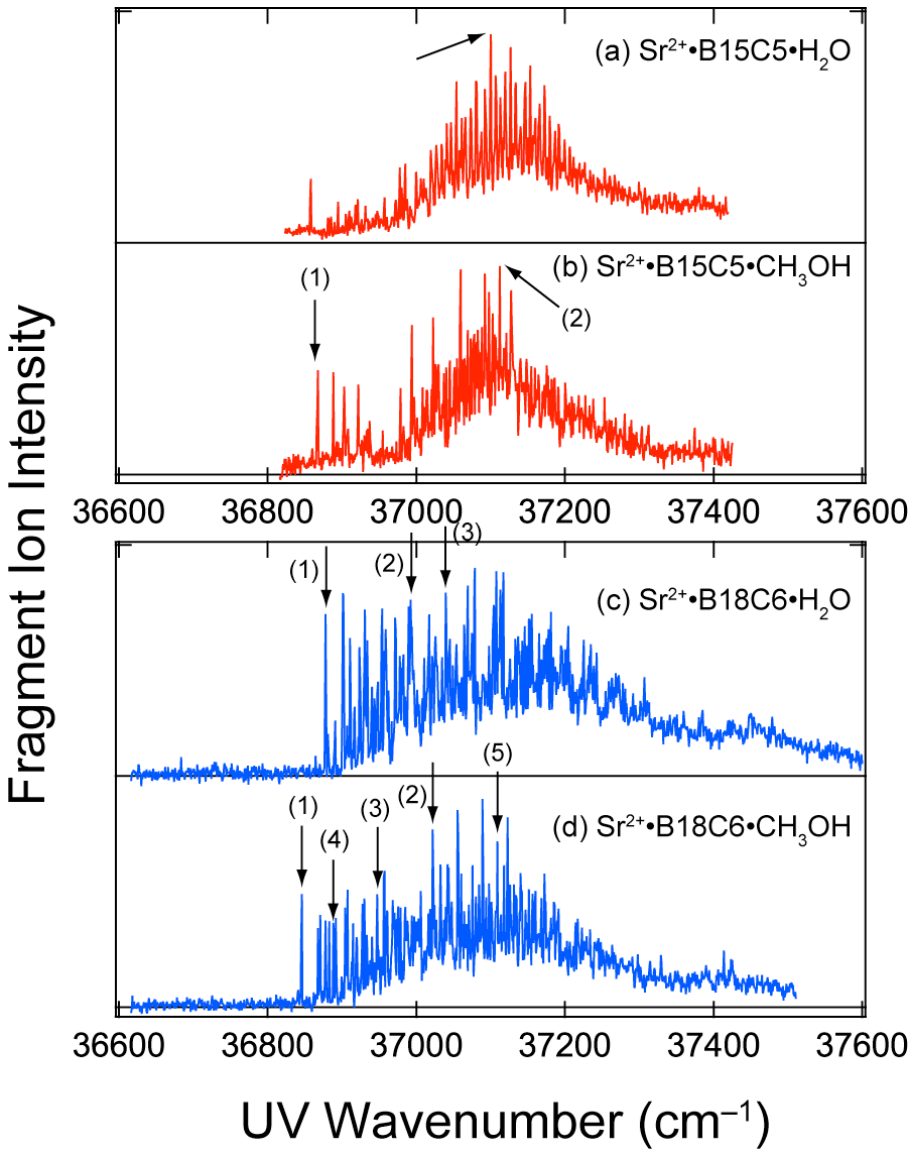

Figure 2. The UVPD spectra of the Sr^{2+} complexes. The arrows show the UV positions at which the IR-UV spectra are measured. The intensity of each spectrum is normalized as having the same maximum intensity for all the spectra.

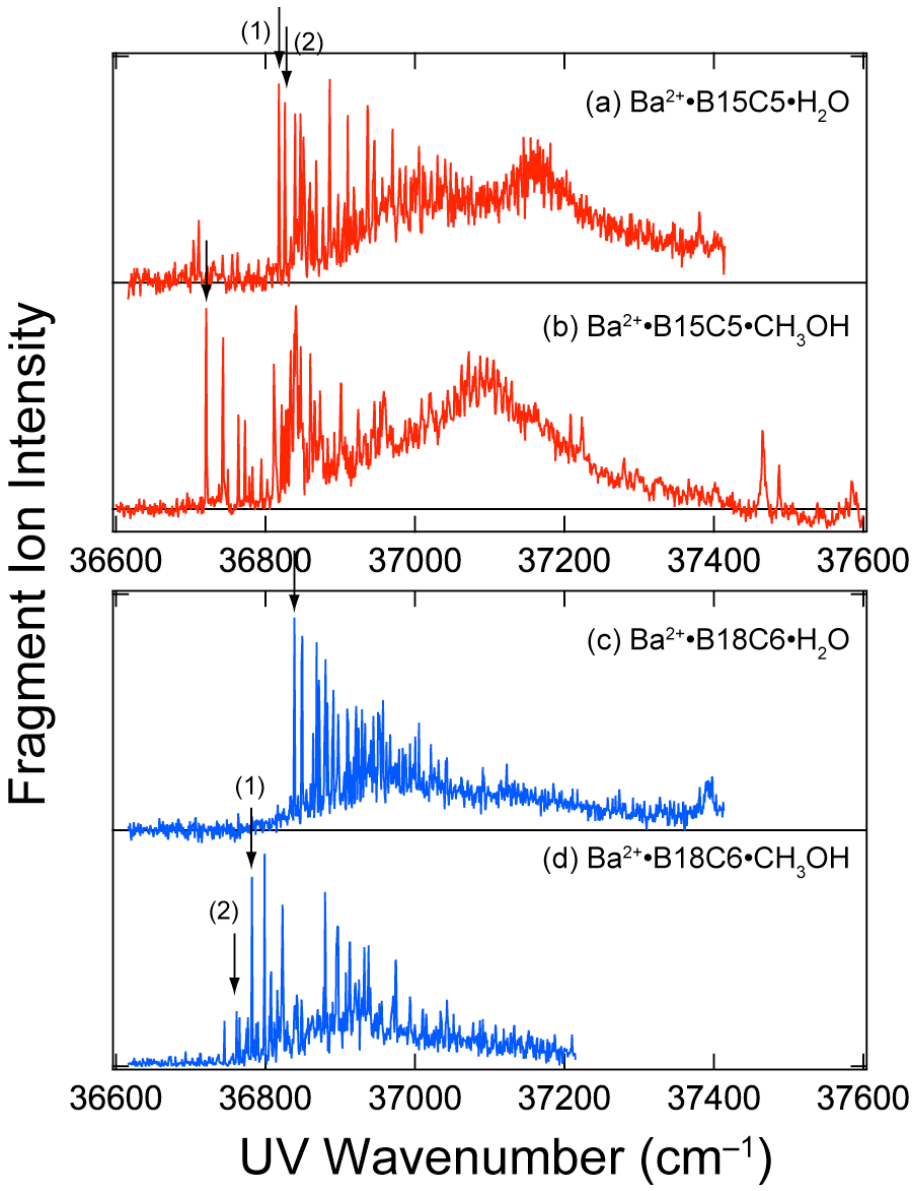

Figure 3. The UVPD spectra of the Ba^{2+} complexes. The arrows show the UV positions at which the IR-UV spectra are measured. The intensity of each spectrum is normalized as having the same maximum intensity for all the spectra.

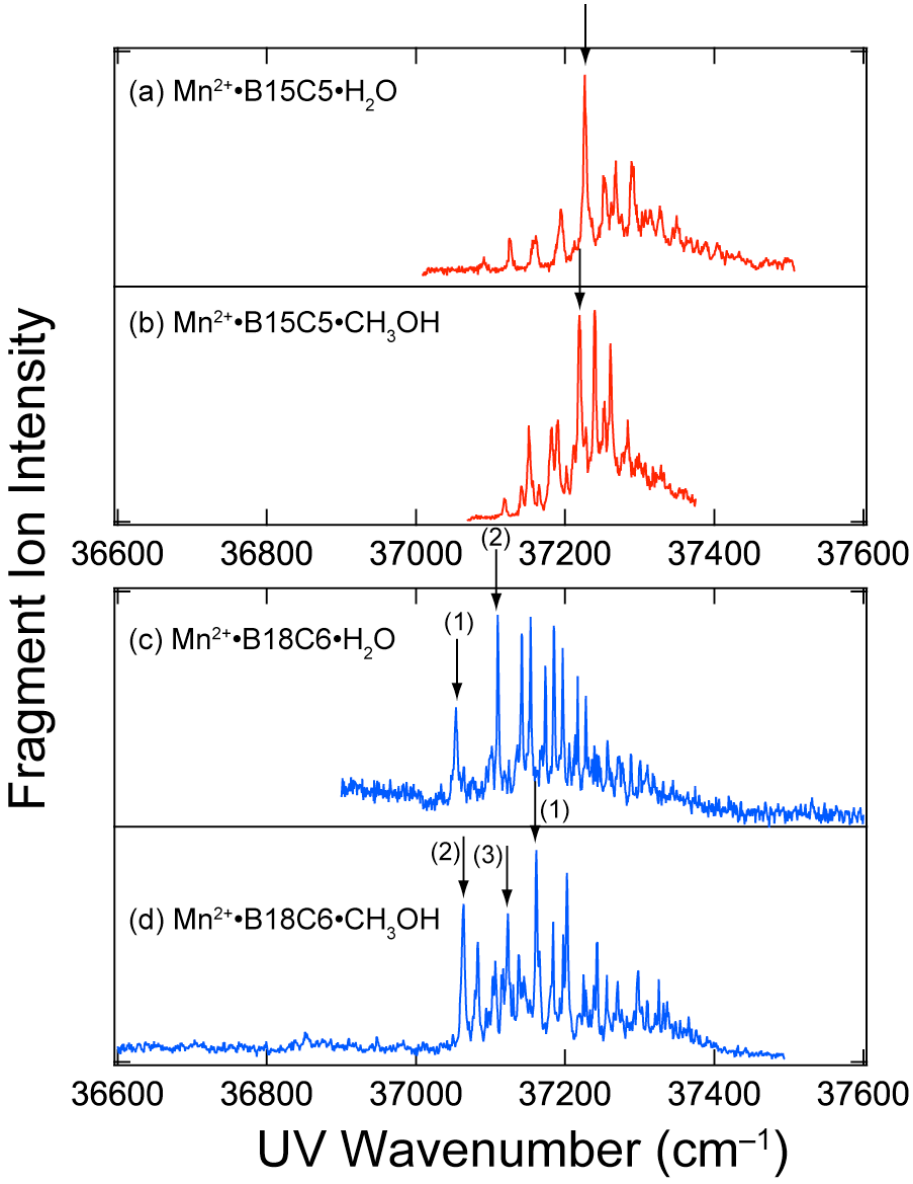

Figure 4. The UVPD spectra of the Mn^{2+} complexes. The arrows show the UV positions at which the IR-UV spectra are measured. The intensity of each spectrum is normalized as having the same maximum intensity for all the spectra.

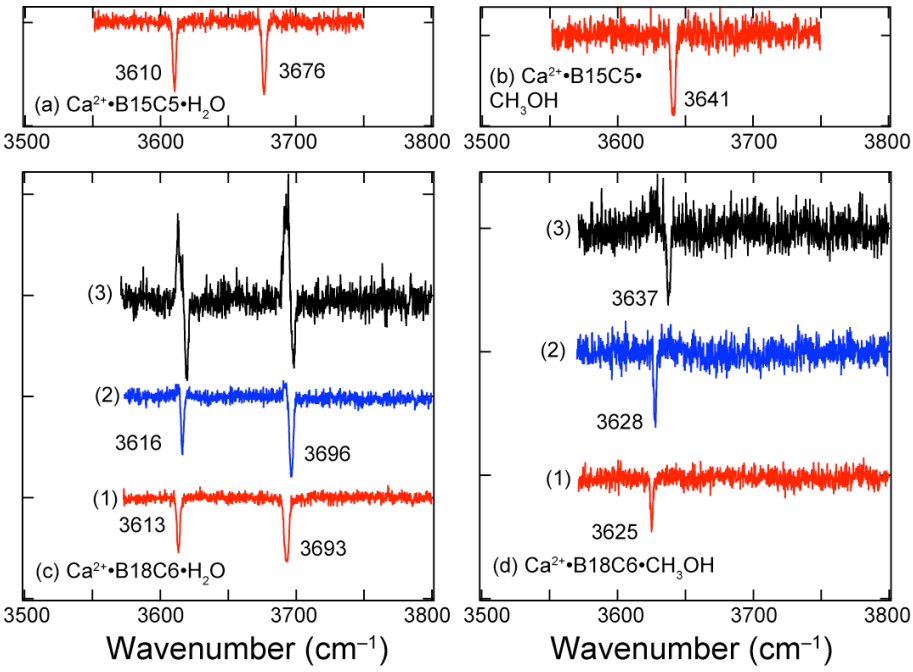

Figure 5. IR-UV double resonance spectra of (a) Ca^{2+}•B15C5•H_2O, (b) Ca^{2+}•B15C5•CH_3OH, (c) Ca^{2+}•B18C6•H_2O, and (d) Ca^{2+}•B18C6•CH_3OH. The numbers in parentheses show the UV position for measuring each IR-UV spectrum (see Fig. 1).

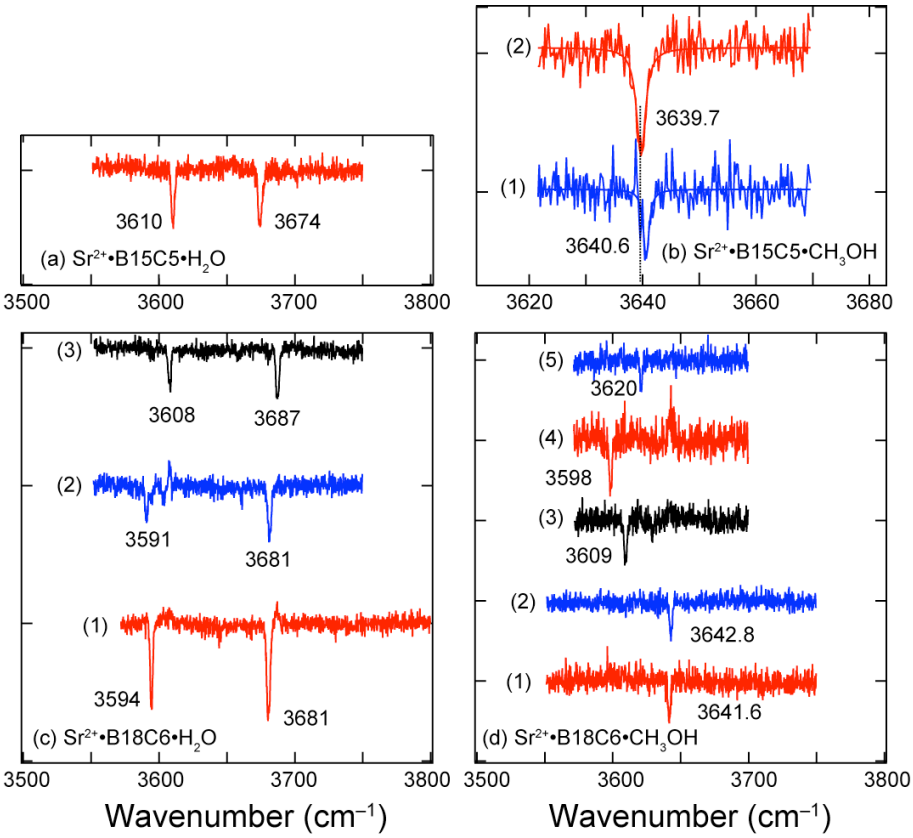

Figure 6. IR-UV double resonance spectra of (a) Sr^{2+}•B15C5•H_2O, (b) Sr^{2+}•B15C5•CH_3OH, (c) Sr^{2+}•B18C6•H_2O, and (d) Sr^{2+}•B18C6•CH_3OH. The numbers in parentheses show the UV position for measuring each IR-UV spectrum (see Fig. 2).

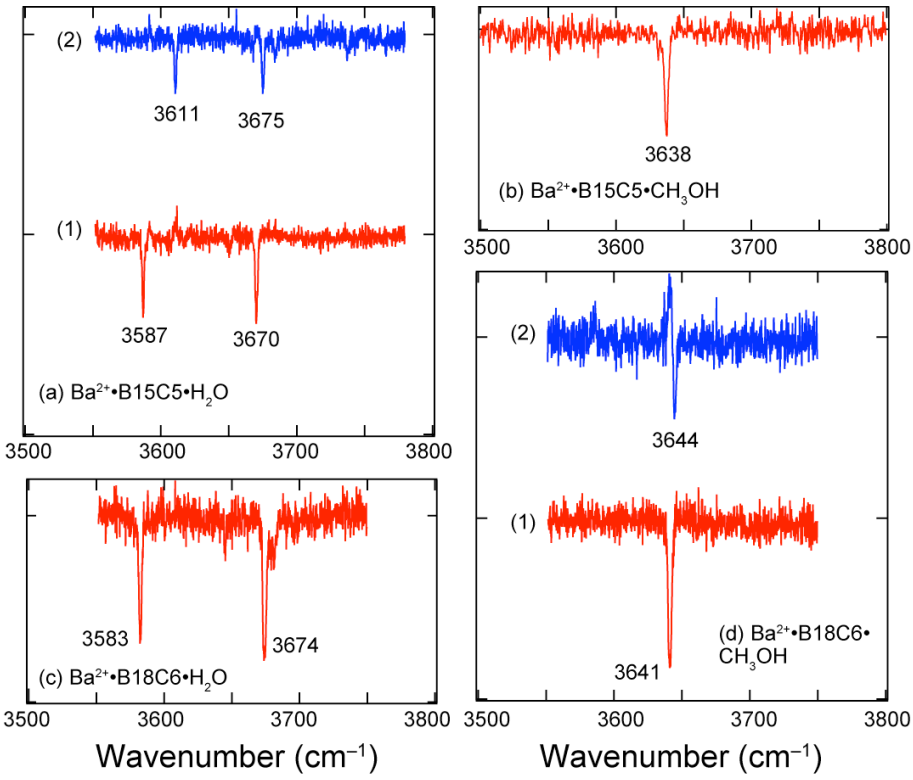

Figure 7. IR-UV double resonance spectra of (a) Ba^{2+}•B15C5•H_2O, (b) Ba^{2+}•B15C5•CH_3OH, (c) Ba^{2+}•B18C6•H_2O, and (d) Ba^{2+}•B18C6•CH_3OH. The numbers in parentheses show the UV position for measuring each IR-UV spectrum (see Fig. 3).

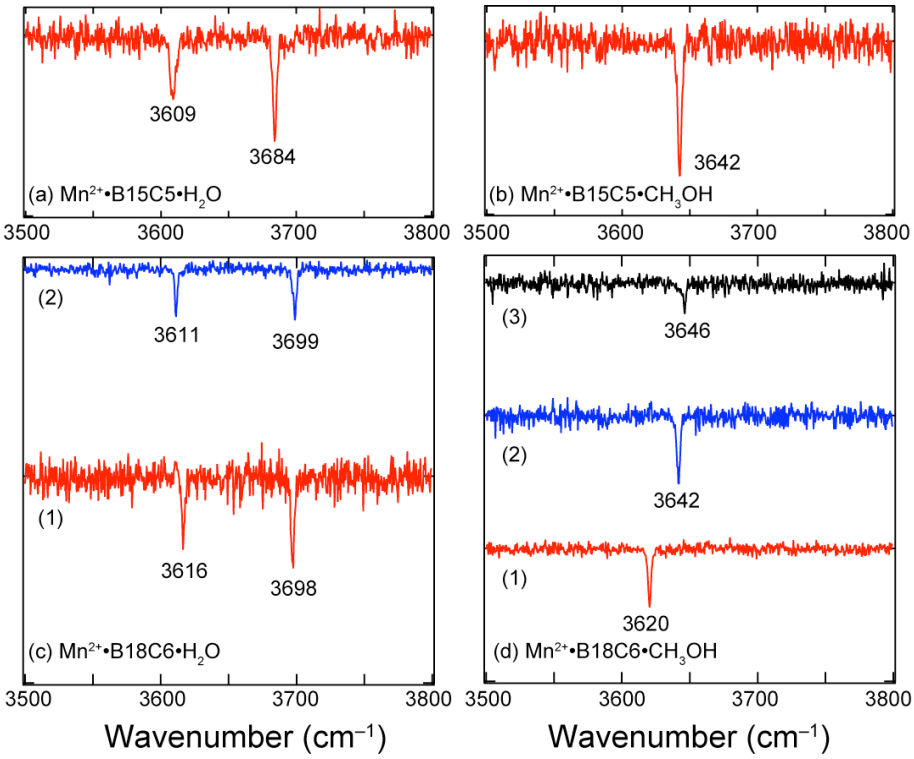

Figure 8. IR-UV double resonance spectra of (a) Mn^{2+}•B15C5•H_2O, (b) Mn^{2+}•B15C5•CH_3OH, (c) Mn^{2+}•B18C6•H_2O, and (d) Mn^{2+}•B18C6•CH_3OH. The numbers in parentheses show the UV position for measuring each IR-UV spectrum (see Fig. 4).

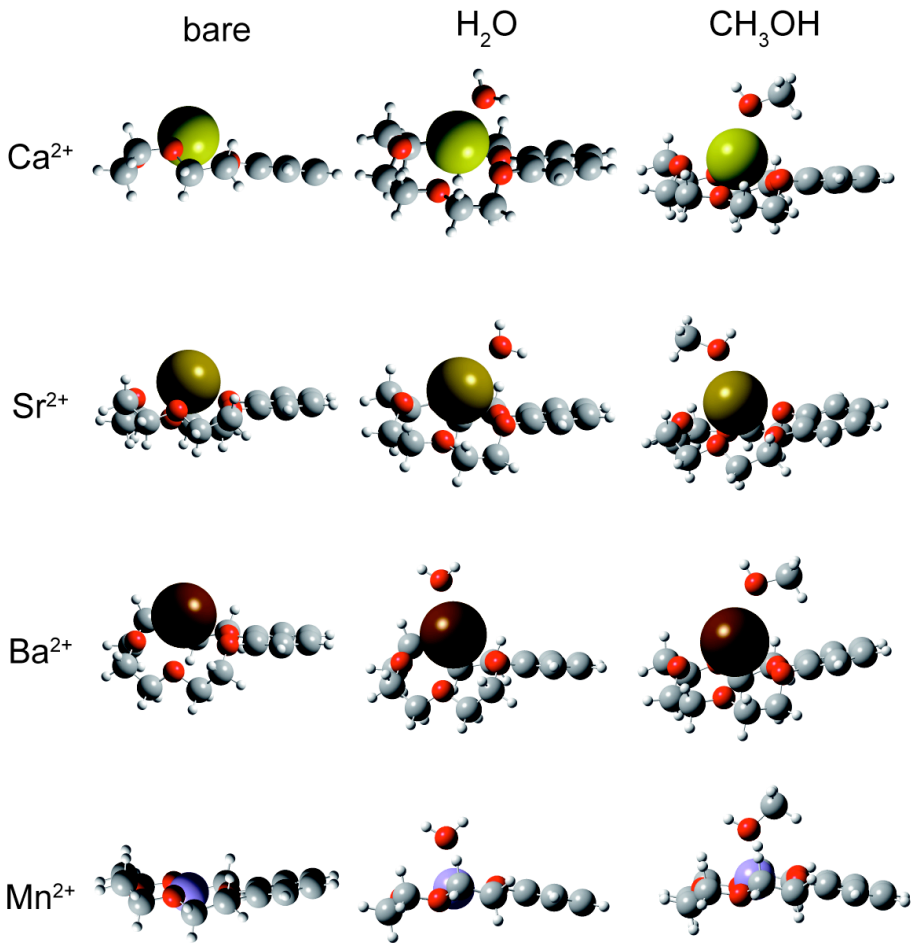

Figure 9. The most stable structures of the B15C5 complexes. The geometry optimizations were performed with the M05-2X/6-31+G(d) level of theory.

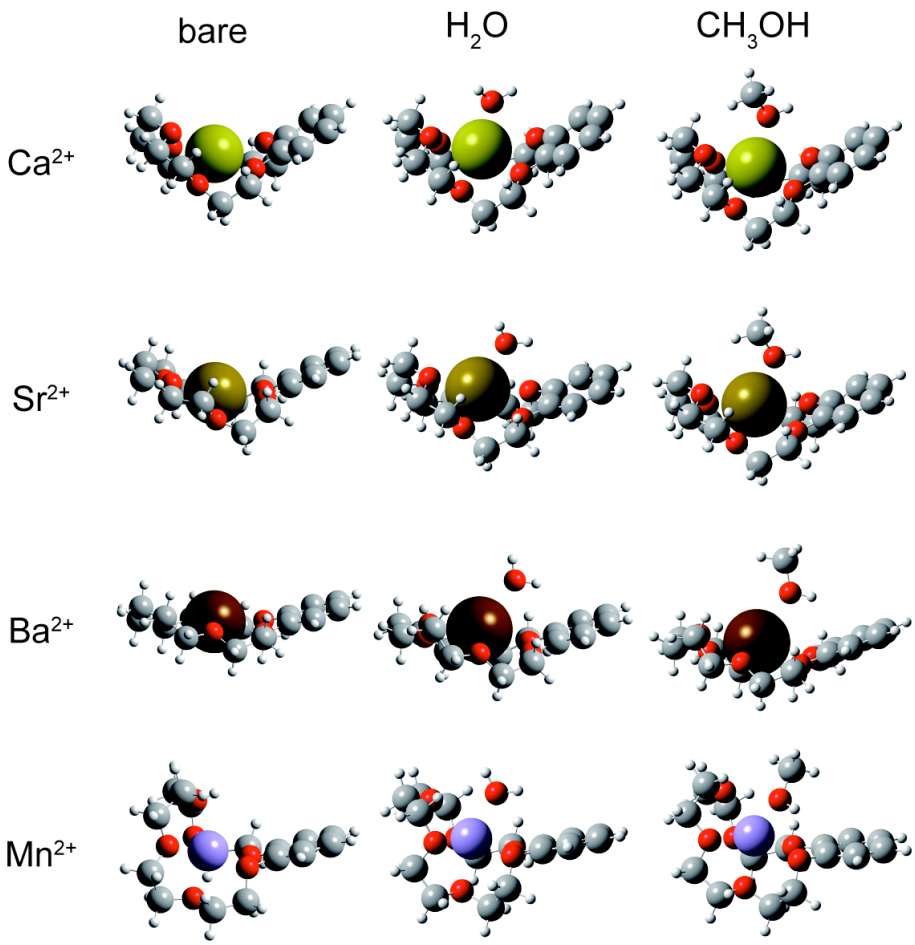

Figure 10. The most stable structures of the B18C6 complexes. The geometry optimizations were performed with the M05-2X/6-31+G(d) level of theory.

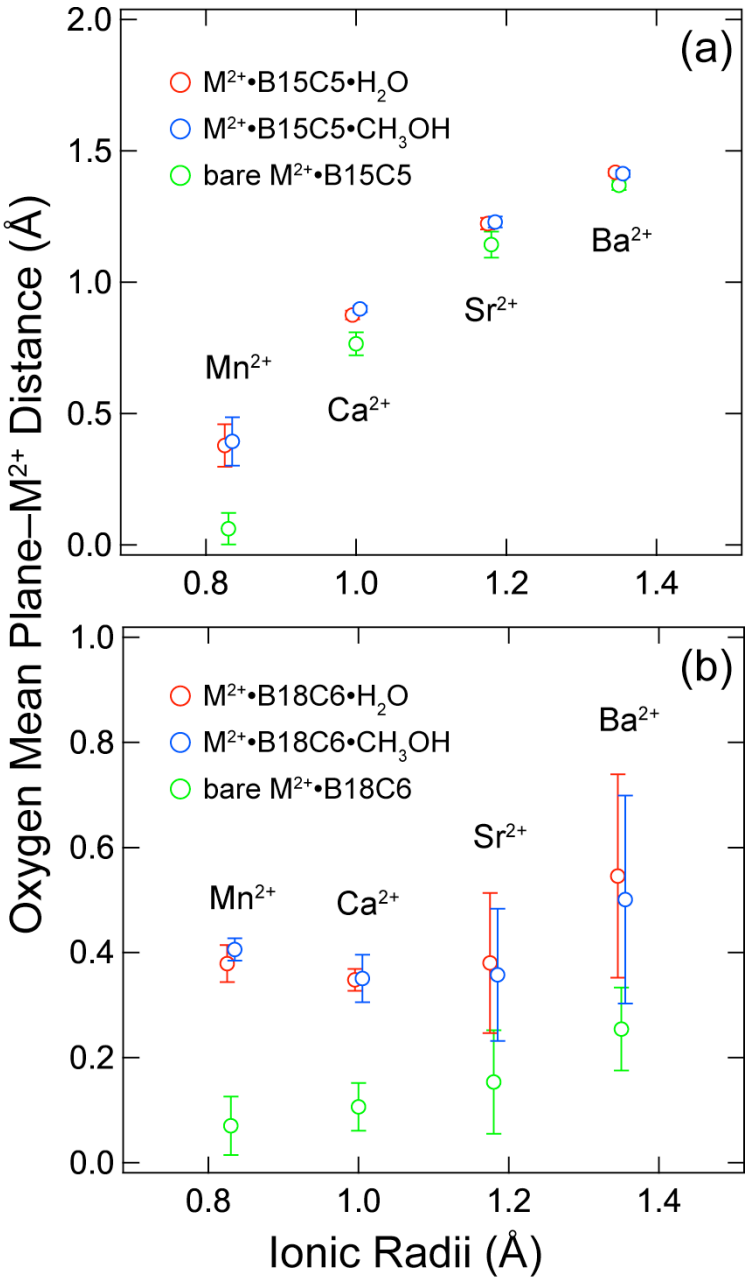

Figure 11. Distance between the mean plane of the oxygen atoms in the ether ring and the M^{2+} ions. These values are obtained for the conformers whose total energy is lower than 5 kJ/mol relative to that of the most stable ones.

Table 1. The number of isomers of M^{2+}•B15C5•L and M^{2+}•B18C6•L complexes with M^{2+} = Ca^{2+}, Sr^{2+}, Ba^{2+}, and Mn^{2+}, and L = H_2O and CH_3OH.

M^{2+}	L = H_2O		L = CH_3OH	
	B15C5	B18C6	B15C5	B18C6
Ca^{2+}	1	3	1	3
Sr^{2+}	1	3	2	5
Ba^{2+}	2	1	1	2
Mn^{2+}	1	2	1	3

References

(1) Izatt, R. M.; Bradshaw, J. S.; Nielsen, S. A.; Lamb, J. D.; Christensen, J. J., Thermodynamic and Kinetic Data for Cation Macrocycle Interaction, *Chem. Rev.* **1985**, *85*, 271-339.

(2) Izatt, R. M.; Terry, R. E.; Haymore, B. L.; Hansen, L. D.; Dalley, N. K.; Avondet, A. G.; Christensen, J. J., Calorimetric Titration Study of Interaction of Several Univalent and Bivalent-Cations with 15-Crown-5, 18-Crown-6, and 2 Isomers of Dicyclohexo-18-Crown-6 in Aqueous-Solution at 25 °C and μ = 0.1, *J. Am. Chem. Soc.* **1976**, *98*, 7620-7626.

(3) Allen, F. H., The Cambridge Structural Database: A Quarter of a Million Crystal Structures and Rising, *Acta Crystallogr. Sect. B: Struct. Sci.* **2002**, *58*, 380-388.

(4) Ray, D.; Feller, D.; More, M. B.; Glendening, E. D.; Armentrout, P. B., Cation-Ether Complexes in the Gas Phase: Bond Dissociation Energies and Equilibrium Structures of Li^+(1,2-Dimethoxyethane)$_X$, x = 1 and 2, and Li^+(12-Crown-4), *J. Phys. Chem.* **1996**, *100*, 16116-16125.

(5) More, M. B.; Ray, D.; Armentrout, P. B., Cation-Ether Complexes in the Gas Phase: Bond Dissociation Energies of Na^+(Dimethyl Ether)$_X$, X=1-4; Na^+(1,2-Dimethoxyethane)$_X$, x =1 and 2; and Na^+(12-Crown-4), *J. Phys. Chem. A* **1997**, *101*, 831-839.

(6) More, M. B.; Ray, D.; Armentrout, P. B., Cation-Ether Complexes in the Gas Phase: Bond Dissociation Energies of K^+(Dimethyl Ether)$_X$, x =1-4; K^+(1,2-Dimethoxyethane)$_X$, x =1 and 2; and K^+(12-Crown-4), *J. Phys. Chem. A* **1997**, *101*, 4254-4262.

(7) More, M. B.; Ray, D.; Armentrout, P. B., Cation-Ether Complexes in the Gas Phase: Bond Dissociation Energies of M^+(Dimethyl Ether)$_X$, x = 1-3, M^+(1,2-Dimethoxyethane)$_X$, x = 1 and 2, and M^+(12-Crown-4) Where M = Rb and Cs, *J. Phys. Chem. A* **1997**, *101*, 7007-7017.

(8) More, M. B.; Ray, D.; Armentrout, P. B., Intrinsic Affinities of Alkali Cations for 15-Crown-5 and 18-Crown-6: Bond Dissociation Energies of Gas-Phase M^+–Crown Ether Complexes, *J. Am. Chem. Soc.* **1998**, *121*, 417-423.

(9) Armentrout, P. B., Cation-Ether Complexes in the Gas Phase: Thermodynamic Insight into Molecular Recognition, *Int. J. Mass spectrom.* **1999**, *193*, 227-240.

(10) Armentrout, P. B.; Austin, C. A.; Rodgers, M. T., Alkali Metal Cation Interactions with 12-Crown-4 in the Gas Phase: Revisited, *Int. J. Mass spectrom.* **2012**, *330*, 16-26.

(11) Zhang, H.; Chu, J. H.; Leming, S.; Dearden, D. V., Gas-Phase Molecular Recognition - Gas-Phase Crown-Ether Alkali-Metal Ion Complexes and Their Reactions with Neutral Crowns, *J. Am. Chem. Soc.* **1991**, *113*, 7415-7417.

(12) Zhang, H.; Dearden, D. V., The Gas-Phase Macrocyclic Effect - Reaction-Rates for Crown Ethers and the Corresponding Glymes with Alkali-Metal Cations, *J. Am. Chem. Soc.* **1992**, *114*, 2754-2755.

(13) Chu, I. H.; Zhang, H.; Dearden, D. V., Macrocyclic Chemistry in the Gas-Phase - Intrinsic Cation Affinities and Complexation Rates for Alkali-Metal Cation Complexes of Crown-Ethers and Glymes, *J. Am. Chem. Soc.* **1993**, *115*, 5736-5744.

(14) Dearden, D. V.; Liang, Y. J.; Nicoll, J. B.; Kellersberger, K. A., Study of Gas-Phase Molecular Recognition Using Fourier Transform Ion Cyclotron Resonance Mass Spectrometry (FTICR/MS), *J. Mass Spectrom.* **2001**, *36*, 989-997.

(15) Anderson, J. D.; Paulsen, E. S.; Dearden, D. V., Alkali Metal Binding Energies of Dibenzo-18-Crown-6: Experimental and Computational Results, *Int. J. Mass spectrom.* **2003**, *227*, 63-76.

(16) Maleknia, S.; Brodbelt, J., Gas-Phase Selectivities of Crown Ethers for Alkali-Metal Ion Complexation, *J. Am. Chem. Soc.* **1992**, *114*, 4295-4298.

(17) Brodbelt, J. S., Probing Molecular Recognition by Mass Spectrometry, *Int. J. Mass spectrom.* **2000**, *200*, 57-69.

(18) Kempen, E. C.; Brodbelt, J. S., A Method for the Determination of Binding Constants by Electrospray Ionization Mass Spectrometry, *Anal. Chem.* **2000**, *72*, 5411-5416.

(19) Lee, S.; Wyttenbach, T.; Vonhelden, G.; Bowers, M. T., Gas-Phase Conformations of Li^+, Na^+, K^+, and Cs^+ Complexed with 18-Crown-6, *J. Am. Chem. Soc.* **1995**, *117*, 10159-10160.

(20) Franski, R., Complexes of Large Crown Ethers with the Lithium Cation Studied by Electrospray Ionization Mass Spectrometry, *Rapid Commun. Mass Spectrom.* **2009**, *23*, 3488-3491.

(21) Franski, R., Cation-π Interactions in Gas-Phase Complexes Formed by Benzo-Crown Ethers and Alkali Metal Cations, *Rapid Commun. Mass Spectrom.* **2011**, *25*, 672-674.

(22) Katritzky, A. R.; Malhotra, N.; Ramanathan, R.; Kemerait, R. C.; Zimmerman, J. A.; Eyler, J. R., Measurement of Gas-Phase Binding-Energies of Crown Ethers with Metal-Ions by Fourier-Transform Ion-Cyclotron Resonance Mass-Spectrometry, *Rapid Commun. Mass Spectrom.* **1992**, *6*, 25-27.

(23) Leize, E.; Jaffrezic, A.; VanDorsselaer, A., Correlation between Solvation Energies and Electrospray Mass Spectrometric Response Factors. Study by Electrospray Mass Spectrometry of Supramolecular Complexes in Thermodynamic Equilibrium in Solution, *J. Mass Spectrom.* **1996**, *31*, 537-544.

(24) Malhotra, N.; Roepstorff, P.; Hansen, T. K.; Becher, J., Alkali-Metal Ion Complexation of Crown Ethers and Related Ligands Studied by Cf-252 Plasma Desorption Mass-Spectrometry, *J. Am. Chem. Soc.* **1990**, *112*, 3709-3710.

(25) Peiris, D. M.; Yang, Y. J.; Ramanathan, R.; Williams, K. R.; Watson, C. H.; Eyler, J. R., Infrared Multiphoton Dissociation of Electrosprayed Crown Ether Complexes, *Int. J. Mass Spectrom. Ion Processes* **1996**, *157*, 365-378.

(26) Schalley, C. A., Supramolecular Chemistry Goes Gas Phase: The Mass Spectrometric Examination of Noncovalent Interactions in Host-Guest Chemistry and Molecular Recognition, *Int. J. Mass spectrom.* **2000**, *194*, 11-39.

(27) Schalley, C. A., Molecular Recognition and Supramolecular Chemistry in the Gas Phase, *Mass Spectrom. Rev.* **2001**, *20*, 253-309.

(28) Rodriguez, J. D.; Lisy, J. M., Infrared Spectroscopy of Gas-Phase Hydrated K^+:18-Crown-6 Complexes: Evidence for High Energy Conformer Trapping Using the Argon Tagging Method, *Int. J. Mass spectrom.* **2009**, *283*, 135-139.

(29) Rodriguez, J. D.; Vaden, T. D.; Lisy, J. M., Infrared Spectroscopy of Ionophore-Model Systems: Hydrated Alkali Metal Ion 18-Crown-6 Ether Complexes, *J. Am. Chem. Soc.* **2009**, *131*, 17277-17285.

(30) Cooper, T. E.; Carl, D. R.; Oomens, J.; Steill, J. D.; Armentrout, P. B., Infrared Spectroscopy of Divalent Zinc and Cadmium Crown Ether Systems, *J. Phys. Chem. A* **2011**, *115*, 5408-5422.

(31) Gamez, F.; Hurtado, P.; Hamad, S.; Martinez-Haya, B.; Berden, G.; Oomens, J., Tweezer-Like Complexes of Crown Ethers with Divalent Metals: Probing Cation-Size-Dependent Conformations by Vibrational Spectroscopy in the Gas Phase, *Chempluschem* **2012**, *77*, 118-123.

(32) Gamez, F.; Hurtado, P.; Martinez-Haya, B.; Berden, G.; Oomens, J., Vibrational Study of Isolated 18-Crown-6 Ether Complexes with Alkaline-Earth Metal Cations, *Int. J. Mass spectrom.* **2011**, *308*, 217-224.

(33) Choi, C. M.; Lee, J. H.; Choi, Y. H.; Kim, H. J.; Kim, N. J.; Heo, J., Ultraviolet Photodepletion Spectroscopy of Dibenzo-18-Crown-6-Ether Complexes with Alkaline Earth Metal Divalent Cations, *J. Phys. Chem. A* **2010**, *114*, 11167-11174.

(34) Inokuchi, Y.; Ebata, T.; Rizzo, T. R.; Boyarkin, O. V., Microhydration Effects on the Encapsulation of Potassium Ion by Dibenzo-18-Crown-6, *J. Am. Chem. Soc.* **2014**, *136*, 1815-1824.

(35) Inokuchi, Y.; Boyarkin, O. V.; Kusaka, R.; Haino, T.; Ebata, T.; Rizzo, T. R., UV and IR Spectroscopic Studies of Cold Alkali Metal Ion-Crown Ether Complexes in the Gas Phase, *J. Am. Chem. Soc.* **2011**, *133*, 12256-12263.

(36) Svendsen, A.; Lorenz, U. J.; Boyarkin, O. V.; Rizzo, T. R., A New Tandem Mass Spectrometer for Photofragment Spectroscopy of Cold, Gas-Phase Molecular Ions, *Rev. Sci. Instrum.* **2010**, *81*, 073107.

(37) Boyarkin, O. V.; Mercier, S. R.; Kamariotis, A.; Rizzo, T. R., Electronic Spectroscopy of Cold, Protonated Tryptophan and Tyrosine, *J. Am. Chem. Soc.* **2006**, *128*, 2816-2817.

(38) Rizzo, T. R.; Stearns, J. A.; Boyarkin, O. V., Spectroscopic Studies of Cold, Gas-Phase Biomolecular Ions, *Int. Rev. Phys. Chem.* **2009**, *28*, 481-515.

(39) Nagornova, N. S.; Rizzo, T. R.; Boyarkin, O. V., Exploring the Mechanism of IR–UV Double-Resonance for Quantitative Spectroscopy of Protonated Polypeptides and Proteins, *Angew. Chem. Int. Ed.* **2013**, *52*, 6002-6005.

(40) Goto, H.; Osawa, E., Corner Flapping: A Simple and Fast Algorithm for Exhaustive Generation of Ring Conformations, *J. Am. Chem. Soc.* **1989**, *111*, 8950-8951.

(41) Goto, H.; Osawa, E., An Efficient Algorithm for Searching Low-Energy Conformers of Cyclic and Acyclic Molecules, *J. Chem. Soc.-Perkin Trans. 2* **1993**, 187-198.

(42) Frisch, M. J.; Trucks, G. W.; Schlegel, H. B.; Scuseria, G. E.; Robb, M. A.; Cheeseman, J. R.; Scalmani, G.; Barone, V.; Mennucci, B.; Petersson, G. A. *et al.*, In *Gaussian 09, Revision A.1*; Gaussian, Inc.: Wallingford CT, 2009.

(43) Schuchardt, K. L.; Didier, B. T.; Elsethagen, T.; Sun, L. S.; Gurumoorthi, V.; Chase, J.; Li, J.; Windus, T. L., Basis Set Exchange: A Community Database for Computational Sciences, *J. Chem. Info. Model.* **2007**, *47*, 1045-1052.

(44) Shubert, V. A.; James, W. H.; Zwier, T. S., Jet-Cooled Electronic and Vibrational Spectroscopy of Crown Ethers: Benzo-15-Crown-5 Ether and 4 '-Amino-Benzo-15-Crown-5 Ether, *J. Phys. Chem. A* **2009**, *113*, 8055-8066.

(45) Kusaka, R.; Inokuchi, Y.; Ebata, T., Water-Mediated Conformer Optimization in Benzo-18-Crown-6-Ether/Water System, *Phys. Chem. Chem. Phys.* **2009**, *11*, 9132-9140.

(46) Inokuchi, Y.; Boyarkin, O. V.; Kusaka, R.; Haino, T.; Ebata, T.; Rizzo, T. R., Ion Selectivity of Crown Ethers Investigated by UV and IR Spectroscopy in a Cold Ion Trap, *J. Phys. Chem. A* **2012**, *116*, 4057-4068.

(47) Lide, D. R. *CRC Handbook of Chemistry and Physics*; 82nd Edition ed.; CRC Press LLC, 2001.

TOC Image